Polycystin promotes renal fibrosis through EZH2

Ming Wu[1,2,3, *#], Yanzhe Wang[1,2,3, *], Ying Jing[4, *], Dongping Chen[1,2,3*], Junyan Lin[1,2,3], Meijie Yuan[1,2,3,5], Bo Tan [6], Di Huang[1,2,3], Chaoyang Ye[1,2,3#]

[1]Department of Nephrology, Shuguang Hospital Affiliated to Shanghai University of Traditional Chinese Medicine

[2]TCM Institute of Kidney Disease of Shanghai University of Traditional Chinese Medicine

[3]Key Laboratory of Liver and Kidney Diseases, Ministry of Education, Shanghai Key Laboratory of Traditional Chinese Clinical Medicine

[4]Department of Nephrology, The 960th Hospital of the PLA Joint Logistics Support Force

[5]Department of Nephrology, The First Hospital of Hebei Medical University, Shijiazhuang 050031，China

[6]Clinical Pharmacokinetic Laboratory, Shuguang Hospital Affiliated to Shanghai University of Traditional Chinese Medicine

*These authors contributed equally to this paper.

Running head: Polycystin promotes renal fibrosis

Corresponding Author1: Prof. Chaoyang Ye, Department of Nephrology, Shuguang Hospital Affiliated to Shanghai University of Traditional Chinese Medicine, No.528 Zhangheng Road, Pudong District, Shanghai 201203, PR China. Fax:

(0086)-21-20256182, E-mail: yechaoyang63@126.com

Corresponding Author 2: Dr. Ming Wu, Department of Nephrology, Shuguang Hospital Affiliated to Shanghai University of Traditional Chinese Medicine, No.528 Zhangheng Road, Pudong District, Shanghai 201203, PR China. Fax: (0086)-21-20256182, E-mail: mingwunl@126.com

Keywords: Polycystin; Renal fibrosis; Triptolide, ADPKD, EZH2

Abstract

Autosomal polycystic kidney disease (ADPKD) is caused by mutations in *PKD1*or *PKD2* gene, which encodes polycystin-1 or polycystin-2 respectively. ADPKD kidneys are progressively enlarged throughout the life which is characterized by increased fibrosis in cystic kidneys. It is still unclear whether the enhanced renal fibrosis in cystic kidneys is the consequence of cyst induced tubular obstruction or a direct result of *PKD* gene mutation. In this study, we determined the role of polycystin in renal fibrosis and explored its underlying mechanisms. We found that the expression of polycystin-1 or polycystin-2 was positively correlated with the expression of collagen-I in the kidney of three different fibrotic mouse models. Pharmaceutical inhibition or genetic knockout of polycystin-2 reduced the expression of pro-fibrotic markers in fibrotic kidneys of two animal models. Moreover, conditional knockout of *Pkd1* gene attenuated renal fibrosis in two mouse models. Enhancer of Zeste homolog 2 (EZH2) is a methyltransferase which plays important role in renal fibrosis. We found that EZH2 was positively correlated with the expression of polycystins in cystic kidneys. Conditional knockout of the *Ezh2* attenuated the anti-fibrotic responses induced by *Pkd1* deletion in fibrotic kidneys.

In conclusion, polycystin promotes renal fibrosis through up-regulation of EZH2 in injured kidneys. Renal fibrosis in polycystic kidneys is not the direct effect of *PKD* gene mutations but the consequence of cyst expansion induced tubular obstruction.

Significance:

Mutations of polycystins cause autosomal polycystic kidney disease (ADPKD) which is associated with increased renal fibrosis in cystic kidneys. However, the role of polycystin in renal fibrosis remains unclear. Here, we showed that the expression of polycystins is positively correlated with the development of renal fibrosis in injured kidneys. Pharmaceutical inhibition or genetic deletion of polycystin-2 attenuated renal fibrosis in fibrotic kidneys. Moreover, genetic deletion of polycystin-1 inhibited renal fibrosis in two different animal models. Finally, we showed that ablation of the methyltransferase EZH2 mitigated the anti-fibrotic effect of polycystin-1 deletion in fibrotic kidneys. We conclude that polycystin promotes through EZH2 and renal fibrosis in cystic kidney is not the direct effect of *PKD* gene mutations.

Introduction

Autosomal polycystic kidney disease (ADPKD) is a leading cause of the end stage renal failure and it is caused by mutations in *PKD1* or *PKD2* gene, which encodes polycystin-1 or polycystin-2 respectively (1). ADPKD is characterized by progressively enlargement of bilateral kidneys which is filled with numerous fluid-filled cysts and associated with massive deposition of interstitial extracellular matrix at the late stage of disease progression (1, 2). Hallmarks of renal fibrosis include overexpression of extracellular matrix fibrils (collagen-I, fibronectin, etc.), up-regulation of epithelial to mesenchymal transition (EMT) markers (a-SMA, vimentin, N-cadherin, etc.), and activation of TGFβ/Smad3 signaling pathway (2, 3). The mechanism of renal fibrosis in ADPKD is largely unexplored (1, 2). Several lines of evidence indicate that genetic defect in *PKD* genes directly induces the production of extracellular matrix proteins (2). However, renal fibrosis in ADPKD kidneys could also be the consequence of cyst growth induced tubular obstruction (1). Indeed, heterozygous deletion of *Pkd1* gene in mice exacerbated fibrosis in the kidney after renal ischemia reperfusion injury and numerous microcysts were observed in injured kidneys of *Pkd1* mice (4). Thus, it is imperative to determine the role of polycystin in renal fibrosis with classical models of renal fibrosis and exclude the interference of cyst induced tubular obstruction.

Polycystin-2 has been identified as a direct target of triptolide, a natural compound extracted from a traditional Chinese herb Lei Gong Teng (5). Through polycystin-2-dependent calcium release, triptolide attenuated disease progression in a

mouse ADPKD model (5). We also showed the beneficial effect of triptolide in human ADPKD patients (6). Besides, triptolide ameliorated proteinuria, attenuated inflammation, and reduced renal fibrosis in several animal models of renal diseases (7, 8). All these data imply that regulation of polycystin-2 activity by triptolide provides renal benefits. In this study, we used triptolide as a molecular probe to study the role of polycystin-2 in renal fibrosis, which was further investigated by using *Pkd2* or *Pkd1* conditional knockout mice and with classic models of renal fibrosis.

Results

The expression of polycystin-2 is increased in three mouse models of renal fibrosis

The time course of polycystin-2 expression was assessed in three different models of renal fibrosis in wild type (WT) mice by Western blotting analysis. Compared with sham kidneys, the expression of polycystin-2 was steadily increased in unilateral ureteral obstruction (UUO) kidneys from day 3, day 7 to day 14, which was correlated with the expression of collagen-I by time (Figure 1A). Similarly, the expression of polycystin-2 was increased in unilateral ischemia-reperfusion injury (UIRI) kidneys from day 3 and reached a peak at day 7 as compared with that in sham kidneys (Figure 1B). The expression of polycystin-2 in UIRI kidneys was positively correlated with the expression of collagen-I by time. Moreover, polycystin-2 was increased by time in aristolochic acid nephropathy (AAN) kidneys from day 7 to day 21 in a same pattern as the expression of collagen-I (Figure 1C).

Triptolide inhibits the expression of polycystin-2 and attenuates fibrosis in fibrotic kidneys

The effect of triptolide on renal fibrosis and the expression of polycystin-2 was evaluated in WT UUO mice. Massive interstitial collagen deposition was observed in UUO kidneys at 10 days after the operation as shown by Masson staining, and treatment with triptolide attenuated collagen deposition (Figure 2A). Increased pro-fibrotic markers such as collagen-I, phosphorylated Smad3 (pSmad3) and a-SMA were detected in UUO kidneys by Western blotting and triptolide reduced the

expression of these pro-fibrotic markers (Figure 2B). Similarly, triptolide inhibited the expression of polycystin-2 in UUO kidneys (Figure 2C).

In UIRI kidneys, triptolide attenuated the deposition of extracellular matrix proteins and reduced the expression of pro-fibrotic markers (collagen-I and a-SMA) (Figure 2D and 2E). In parallel, triptolide blocked the elevated expression of polycystin-2 in UIRI kidneys (Figure 2F).

Triptolide inhibits renal fibrosis through down-regulation of polycystin-2

The anti-fibrotic effect of triptolide was further confirmed *in vitro* using TGF-β stimulated human renal epithelial (HK2) cells or normal rat kidney fibroblast (NRK-49F) cells. Triptolide dose-dependently inhibited the expression of pro-fibrotic markers (fibronectin, N-cadherin, vimentin, and pSmad3) in TGF-β stimulated HK2 cells from 100 nM to 1000 nM (Figure 3A). Similarly, the expression of pro-fibrotic markers (fibronectin, N-cadherin, and vimentin) were dose-dependently inhibited by triptolide in NRK-49F cells from 100 nM to 1000 nM (Figure 3B). The expression of polycystin-2 was also dose-dependently inhibited by triptolide in TGF-β stimulated HK2 cells or NRK-49F cells from 100 nM to 1000 nM (Figure 3A and 3B).

As shown by Figure 3C and 3D, PKD2 siRNA inhibited the expression of polycystin-2 in normal or TGF-β stimulated HK2 cells, which was correlated with down-regulation of pro-fibrotic markers (fibronectin, N-cadherin, vimentin, and pSmad3). We further showed that triptolide inhibited the expression of polycystin-2 and pro-fibrotic markers (fibronectin, N-cadherin, vimentin, and pSmad3) in PKD2 knockdown HK2 cells in a less extent than that in non-sense control (NC) siRNA

transfected HK2 cells (Figure 3E).

Conditional knockout of *Pkd2* gene mitigates renal fibrosis in mouse UUO kidneys

To further confirmed the pro-fibrotic effect of polycystin-2, we generated *Pkd2* conditional knockout mice. Heterozygous (*Pkd2*$^{fl/+}$*;Cre/Esr1*$^{+}$) or homozygous (*Pkd2*$^{fl/fl}$*;Cre/Esr1*$^{+}$) conditional knockout of *Pkd2* reduced positive areas of Masson-staining in UUO kidneys (Figure 4A). Dilated tubules were observed in control (*Pkd2*$^{fl/+}$*;Cre/Esr1*$^{-}$) or heterozygous *Pkd2* knockout UUO kidneys (Figure 4A). Interestingly, numerous small cysts (luminal diameter exceeding 50 μm) were observed in homozygous *Pkd2* knockout mice (Figure 4A). Western blotting analysis further showed that heterozygous or homozygous conditional knockout of *Pkd2* inhibited the expression of polycystin-2 and pro-fibrotic markers (collagen-I, pSmad3, and a-SMA) (Figure 4B).

Polycystin-1 is increased in fibrotic kidneys and conditional deletion of *Pkd1* gene attenuates renal fibrosis in mouse kidneys

The expression of polycystin-1, the counterpart of polycystin-2, was measured in the UUO model of renal fibrosis in WT mice. Compared with sham kidneys, the expression of polycystin-1 was increased from day 3 to day 14 in UUO kidneys (Figure 5A).

Using *Pkd1* conditional knockout mice, we found that heterozygous (*Pkd1*$^{fl/+}$*;Cre/Esr1*$^{+}$) or homozygous (*Pkd1*$^{fl/fl}$*;Cre/Esr1*$^{+}$) conditional knockout of *Pkd1* gene reduced the content of extracellular matrix in UUO kidneys as shown by

Masson staining (Figure 5B). Numerous small cysts were observed in homozygous *Pkd1* knockout mice (Figure 5B). Heterozygous or homozygous conditional knockout of *Pkd1* inhibited the expression of polycystin-1 and pro-fibrotic markers (collagen-I, pSmad3, and a-SMA) in UUO kidneys as compared with control ($Pkd1^{fl/+}$;$Cre/Esr1^{-}$) UUO kidneys (Figure 5C). The effect of *Pkd1* on renal fibrosis was further evaluated in folic acid (FA) induced nephropathy. Intraperitoneal injection of FA for 48h increased the accumulation of extracellular matrix and up-regulation of pro-fibrotic markers (collagen-I, pSmad3, and a-SMA) in control ($Pkd1^{fl/+}$;$Cre/Esr1^{-}$) mouse kidneys (Figure 5D and 5E). Heterozygous deletion of *Pkd1* ($Pkd1^{fl/+}$;$Cre/Esr1^{+}$) reduced extracellular matrix deposition and expression of pro-fibrotic markers in FA kidneys (Figure 5D and 5E).

Polycystins promote renal fibrosis through EZH2

Enhancer of zeste 2 (EZH2) is an important epigenetic regulator during the development of renal fibrosis (9). EZH2 was upregulated in mouse UUO kidneys as compared with sham kidneys in control mice (Figure 6A and 6B). We found that heterozygous or homozygous conditional knockout of *Pkd2* or *Pkd1* gene dose-dependently inhibited the expression of EZH2 in mouse UUO kidneys (Figure 6A and 6B). Upregulation of EZH2 was also observed in FA kidneys in control mice, which was inhibited by heterozygous deletion of *Pkd1* gene (Figure 6C). Conditional knockout of *Ezh2* reduced extracellular matrix deposition and the expression of pro-fibrotic markers (collagen-I, pSmad3, and a-SMA) in UUO kidneys (Figure 6D and 6E). Inhibition of extracellular matrix deposition or the expression of pro-fibrotic

markers (collagen-I, pSmad3, and a-SMA) by *Pkd1* deletion in *Ezh2* knockout kidneys (*Ezh2*$^{fl/fl}$*;Pkd1*$^{fl/fl}$*;Cre/Esr1*$^{+}$) was less than that in *Ezh2* control kidneys (*Ezh2*$^{+/+}$*; Pkd1*$^{fl/fl}$*;Cre/Esr1*$^{+}$), suggesting that polycystins promote renal fibrosis through EZH2 (Figure 6D and 6E).

Discussion

Deletion of polycystin-1 or polycystin-2 is associated with renal fibrosis in humans and animal models with cystic phenotype, implying that polycystins are anti-fibrotic proteins in diseased kidneys (2, 10). However, renal fibrosis in cystic kidneys can also be induced by tubular obstruction which is caused by cyst expansion (1). To determine the role of polycystins in renal fibrosis, we first measured the expression of polycystin-2 in fibrotic kidneys in WT mice. We found that polycystin-2 was up-regulated in three different mouse model of renal fibrosis in a time-dependent manner, which was positively correlated with the expression of collagen-I. Next, we used triptolide as a molecular probe to determine the role of polycystin-2 in renal fibrosis. We found that triptolide inhibited the expression of polycystin-2 in fibrotic kidneys, which was correlated with reduced interstitial collagen deposition and reduced expression of pro-fibrotic markers in injured kidneys. In two *in vitro* models, we further showed that triptolide dose-dependently reduced the expression of polycystin-2 and pro-fibrotic markers. Finally, we showed that knockdown of *PKD2* gene attenuated the inhibitory effect of triptolide on the expression of pro-fibrotic markers in TGF-β stimulated HK2 cells. Thus, we conclude that inhibition of polycystin-2 by triptolide attenuates renal fibrosis.

To confirm this finding, we generated a *Pkd2* conditional knockout mice. We showed that heterozygous or homozygous deletion of *Pkd2* inhibited the expression of pro-fibrotic markers and extracellular matrix deposition in UUO kidneys. Polycystin-1 is the counterpart of polycystin-2, which shares common downstream

signaling pathways leading to the same biological outcome (11). We further showed that conditional knockout of *Pkd1* gene reduced pro-fibrotic marker expression and collagen accumulation in fibrotic kidneys induced by UUO operation or FA injection. In conclusion, polycystins are pro-fibrotic proteins in injured kidneys.

In adult mice, renal cysts can be induced upon injuries in *Pkd* gene homozygous conditional knockout mice (12, 13). To exclude the effect of cyst formation on renal fibrosis, we included *Pkd* gene heterozygous conditional knockout mice in our study and no renal cyst was observed in injured kidney after *Pkd* gene heterozygous deletion. In our study, we observed numerous small cysts formed in homozygous knockout mice at two weeks after the UUO surgery. Surprisingly, collagen deposition is almost absent in homozygous knockout UUO mice indicating that *Pkd* gene deletion can inhibit renal fibrosis at very early stage of cyst formation.

A previous study showed that increased fibrosis was observed in *Pkd2* heterozygous mouse kidneys after UIRI operation as compared with that in WT kidneys (14). However, this experiment was performed in 4-6 months old *Pkd2* gene heterozygous conventional knockout mice where the baseline tubular proliferation in heterozygous kidneys was significantly higher than that in WT kidneys (14). To have the same baseline condition, we only inactivated *Pkd* gene at one week before the UUO operation or FA injection.

Polycystin-2 is up-regulated in kidneys upon ischemic or toxic acute injury, which was thought to be a protective mechanism for injured kidneys (15). Interestingly, overexpression of renal polycystin-2 was also observed in non-orthologous rodent

model of PKD (15). Surprisingly, up-regulation of polycystin-2 and even its partner protein polycystin-1 were observed in human ADPKD kidney samples by different labs over two decades ago (16). However, there is still no clear scientific explanation for these observations. Here, we showed that polycystin-1 or polycystin-2 is up-regulated in UUO kidneys, suggesting that up-regulation of polycystins in human ADPKD kidneys is a fibrotic response of cyst growth induced tubular obstruction.

A very recent report showed that re-expression of polycystin-1 or polycystin-2 reversed the disease progression in *PKD* gene knockout mice suggesting that ADPKD is reversible once polycystin dosage is adjusted to normal levels (17). However, the situation in human ADPKD kidneys is more complicated than that in ADPKD mouse kidneys. According to the 'two-hit' theory, renal cyst is originated from tubular cells with a second somatic mutation (second hit) (13). Delivery of excessive exogenous polycystins to tubular cells without a second hit may cause overtreatment and even promote renal fibrosis. In the study by Dong *et al.*, the exogenous polycystin-2 expression was 1.5-fold higher than endogenous levels of polycystin-2, which was probably still at the physiological levels when it was re-expressed in Pkd2 null animals. In our study, we found that tubular obstruction by UUO operation induced 28.9 times higher expression of polycystin-2 in the kidney at day 3, which was correlated with 9.1-fold higher expression of collagen-I suggesting that a pathological high dosage of polycystin-2 is pro-fibrotic in diseased kidneys. Thus, genetic re-expression of polycystins in human ADPKD kidneys should be precisely designed to target specific renal cells with controlled dosage.

EZH2 is an important epigenetic regulator during the development of renal fibrosis and has been intensively studied in recent years (9, 18). We hypothesized that polycystins promote renal fibrosis through EZH2. In the current study, we found that EZH2 expression is positively correlated with the expression of polycystins in fibrotic kidneys. Genetic deletion of polycystins reduced the expression of EZH2 in fibrotic kidneys. Importantly, genetic knockout of *Ezh2* attenuated the anti-fibrotic effect of *Pkd1* deletion in UUO kidneys. Thus, we conclude that polycystin promotes renal fibrosis through up-regulation of EZH2.

Our study not only revealed the role of polycystins in renal fibrosis but also shed lights on the mechanism of renal fibrosis in ADPKD. We suggest that future genetic therapy to ADPKD patients should be precisely designed to control the dosage of exogenous polycystins.

Materials and Methods

Animals

Only male mice were used in animal studies. Wide type (WT) C57BL/6 mice (SPF grade, 20-25g) were purchased from Shanghai SLAC Laboratory Animal Co., Ltd. *Pkd1*$^{fl/fl}$ mice were obtained from Prof. Rudolf Wüthrich in University of Zurich, which were originally from the lab of Professor Gregory Germino in Johns Hopkins University School of Medicine (19). C57/BL6 *Pkd1*$^{fl/fl}$ mice were crossed with C57/BL6 tamoxifen-Cre (B6. Cg-Tg [Cre/Esr1]) 5Amc/J mice (stock 004682; Jackson Laboratories) as described previously (20). *Ezh2*$^{fl/fl}$ mice on a C57/B6 background were provided by Prof. Xi Wang from Capital Medical University and were further crossed with *Pkd1*$^{fl/fl}$*;Cre/Esr1*$^{+}$ mice (21). *Pkd2* conditional knockout mice with exon 3 deletion have cystic phenotype in the kidney (22). CRISPR/Cas9 technology was used to generate a mouse with loxP sites flanking exon 3 of the Pkd2 gene by Shanghai Model Organisms Center. *Pkd2*$^{fl/fl}$ were crossed with tamoxifen-Cre mice to generate *Pkd2*$^{fl/fl}$*;Cre/Esr1*$^{+}$ mice. Animals were housed in the animal facility of Shanghai University of Traditional Chinese Medicine according to local regulations and guidelines. Animal experiments were approved by the ethic committee of Shanghai University of Traditional Chinese Medicine (PZSHUTCM18102604).

Genotyping

Genomic DNA was prepared from mouse tail by using animal genomic DNA quick extraction kit (D0065M, Beyotime Biotech, Nantong, China) as described in the manufacturer's instructions. PCR genotyping was performed using the following primers: Pkd2-F, GTACACCTGTGCAGCACTCA; Pkd2-R,

GGAGCTCATCATGCCGTAGG; CRE-F, ATTGCTGTC ACTTGGTCGTGGC; CRE-R, GGAAAATGCTTCTGTCCGTTTGC; Pkd1-F, CCTGCCTTGCTCTACTTTCC; PKD1-R, AGGGCTTTTCTTGCTGGTCT; EZH2-F, CCCATGTTTAAGGGCATAGTGACATG; EZH2-R, ATGTGCAGGTCAGTCAGCAACTTCAG. Details regarding PCR conditions are available upon request.

Experimental Animal Protocol

UUO operation was performed through twice ligation of the left ureter with 4-0 nylon sutures. WT animals were sacrificed at day 3, 7 or 14 in a time-course experiment (n=5 for each time point). For interventional study, WT mice were randomly divided into four groups: 1) Sham/Vehicle (n=6), 2) Sham/triptolide (n=7), 3) UUO/ Vehicle (n=7), and 4) UUO/triptolide (n=7) group. The stock of triptolide (Topscience, T2179, Shanghai, China) was dissolved in DMSO and further diluted in normal saline as working solution. Sham or UUO mice were treated with vehicle or 0.25 mg/kg triptolide daily by intraperitoneal (i.p.) injection for 10 days starting from day 0. Mice were sacrificed at day 10. Kidney samples were obtained for Western blotting analysis or histological examinations. For conditional knockout mice (n= 7-9 mice per group), Cre recombinase activity was induced by intraperitoneally injection of tamoxifen (50 mg kg^{-1} day^{-1}, Apexbio, B5965) for three consecutive days at one week before UUO operations. Conditional knockout mice at 8 weeks of age were subjected to UUO operation and were sacrifice at day14.

For the UIRI model, left renal pedicles were clamped for 35 minutes using

microaneurysm clamps in male mice. WT animals were sacrificed at day 3, 7 or 14 in a time-course experiment (n=5 for each time point). For interventional study, WT mice were randomly divided into three groups (n= 6-7 mice per group) and were treated with vehicle or 0.25 mg/kg triptolide daily by i.p. injection starting from day 1 for 10 days. Mice were sacrificed at day 11.

To induce aristolochic acid nephropathy in mice, aristolochic acid I (AAI, A9451, Sigma; 5 mg/kg body weight) or normal saline (NS) was peritoneally injected once. WT animals were sacrificed at day 3, 7 or 21 in a time-course experiment (n=5 for each time point). Kidney tissues were collected.

To establish folic acid (FA)-induced nephropathy, mice at 6-8 weeks of age were injected intraperitoneally with FA (F7876, Sigma-Aldrich, dissolved in 0.3M sodium bicarbonate at a dose of 250 mg/kg). Sodium bicarbonate alone was used as controls. For conditional knockout mice (n= 9 mice per group), Pkd gene inactivation was induced by intraperitoneally injection of tamoxifen for three consecutive days at one week before FA injection. Kidney samples were collected at 48h after FA administration for further analysis.

Cell Culture

Normal rat kidney 49F (NRK-49F) cells, a rat kidney interstitial fibroblast cell line, were purchased from national infrastructure of cell line resource, Chinese academy of medical sciences. To study the anti-fibrotic effect of triptolide, NRK-49F cells were seeded in 6-well plates to 40–50% confluence and were starved with DMEM/F12 medium containing 0.5% fetal bovine serum overnight before the

experiment. The next day, cells were refreshed with 0.5%medium and then were exposed to different concentrations of triptolide (10 nM, 100 nM, and 1000 nM) for 24h. Protein was extracted from cell lysates for further analysis.

HK2 renal proximal tubular epithelial cells were obtained from the Cell Bank of Shanghai Institute of Biological Sciences (Chinese Academy of Science). HK2 cells were seeded in 6-well plate to 40-50% confluence, which were starved overnight with DMEM/F12 medium containing 0.5% fetal bovine serum. On the next day, fresh medium containing 0.5% fetal bovine serum was changed, and then cells were exposed to 2.5 ng/ml TGF-β (Peprotech, Rocky Hill, NJ, USA) for 48h in the presence of various concentration of triptolide.

Nonsense control (NC) or human PKD2 siRNA were transfected by Lipofectamine 2000 (11668-027; Invitrogen) in HK2 cells using DMEM/F12 medium containing 10% fetal bovine serum according to the manufacturer's instruction. Protein was extracted from cell lysates at 24h after transfection. In another experiment, fresh medium containing 0.5% fetal bovine serum was changed in the second day after transfection, and then cells were exposed to 2.5 ng/ml TGF-β (Peprotech, Rocky Hill, NJ, USA) for 48h with or without triptolide. The NC siRNA sequences were as follows: forward, 5′-UUCUCCGAACGUGUCACGUTT-3′; and reverse, 5′-ACGUGACACGUUCGGAGAATT-3′. The human PKD2 siRNA sequences were as follows: forward, 5′-GGACAUAGCUCCAGAAGGATT-3′; and reverse, 5′-UCCUUCUGGAGCUAUGUCCTT-3′.

Masson's Trichrome Staining

Mouse kidneys were fixed and embedded in paraffin. Four-μm-thick sections of paraffin-embedded kidney tissue was stained with hematoxylin, and then with ponceau red liquid dye acid complex, which was followed by incubation with phosphomolybdic acid solution. Finally, the tissue was stained with aniline blue liquid and acetic acid. Images were obtained with the use of a microscope (Nikon 80i, Tokyo, Japan).

Western Blotting Analysis

Cell or kidney protein was extracted by using lysis buffer bought from Beyotime Biotech (P0013, Nantong, China). The protein concentration was measured by using BCA Protein Assay Kit (P0012S, Beyotime Biotech, Nantong, China). Protein samples were dissolved in 5x SDS-PAGE loading buffer (P0015L, Beyotime Biotech, Nantong, China), which were further subjected to SDS-PAGE gel electrophoresis. After electrophoresis, proteins were electro-transferred to a polyvinylidene difluoride membrane (Merck Millipore, Darmstadt, Germany), which was incubated in the blocking buffer (5% non-fat milk, 20mM Tris-HCl, 150mMNaCl, PH=8.0, 0.01%Tween 20) for 1 hour at room temperature and was followed by incubation with anti-polycystin-1 (1:500, sc-130554, SantaCruz), anti-polycystin-2 (1:1000, 19126-1-AP, Proteintech), anti-polycystin-2 (1:1000, A3625, ABclonal), anti-EZH2 (1:1000, 5246S, Cell Signaling Technology) antibody, anti-fibronectin (1:1000, ab23750, Abcam), anti-pSmad3 (1:1000, ET1609-41, HUABIO), anti-Collagen I (1:1000, ab260043, Abcam), anti-α-SMA (1:1000, ET1607-53, HUABIO), anti-N-cadherin (1:1000, sc-59887, Santa Cruz), anti-vimentin (1:1000, R1308-6,

HUABIO), anti-GAPDH (1:5000, 60004-1-lg, Proteintech), or anti-α-tubulin (1:1000, AF0001, Byotime) antibodies overnight at 4□. Binding of the primary antibody was detected by an enhanced chemiluminescence method (SuperSignal™ West Femto, 34094, Thermo Fisher Scientific) using horseradish peroxidase-conjugated secondary antibodies (goat anti-rabbit IgG, 1:1000, A0208, Beyotime or goat anti-mouse IgG, 1:1000, A0216, Beyotime).

Statistical Analysis

Statistical analyses were performed by one-way ANOVA followed by a Dunnett's multiple comparisons test using GraphPad Prism version 5.0 (GraphPad, San Diego, CA). All data are expressed as means ± SD, and $P < 0.05$ was considered as statistically significant.

Conflict of Interest Statement

The authors have no conflicts of interest to declare.

Funding Sources

This work was supported by Key Disciplines Group Construction Project of Pudong Health Bureau of Shanghai (PWZxq2017-07); The Three Year Action Plan Project of Shanghai Accelerating Development of Traditional Chinese Medicine (ZY(2018-2020)-CCCX-2003-08); Shanghai Key Laboratory of Traditional Chinese Clinical Medicine (20DZ2272200), Shanghai, PR China; Scientific Research Foundation of Shanghai Municipal Commission of Health and Family Planning (201740193) to MW; National Natural Science Foundation of China (81873617; 82170747) to CY.

Author Contributions

CY funded the project. MW, YJ, CY, DC conceived and coordinated the study. MW wrote the paper. MW and YW conducted the *in vitro* experiments. MW, YW, YJ, JL, DC, BT, MY and DH performed the animal experiments. YW performed and analyzed the Western blotting. All authors reviewed the results and approved the final version of the manuscript.

References

1. Grantham JJ, Mulamalla S, & Swenson-Fields KI (2011) Why kidneys fail in autosomal dominant polycystic kidney disease. *Nat Rev Nephrol* 7(10):556-566.

2. Song CJ, Zimmerman KA, Henke SJ, & Yoder BK (2017) Inflammation and Fibrosis in Polycystic Kidney Disease. *Results Probl Cell Differ* 60:323-344.

3. De Chiara L & Crean J (2016) Emerging Transcriptional Mechanisms in the Regulation of Epithelial to Mesenchymal Transition and Cellular Plasticity in the Kidney. *J Clin Med* 5(1).

4. Bastos AP*, et al.* (2009) Pkd1 haploinsufficiency increases renal damage and induces microcyst formation following ischemia/reperfusion. *J Am Soc Nephrol* 20(11):2389-2402.

5. Leuenroth SJ*, et al.* (2007) Triptolide is a traditional Chinese medicine-derived inhibitor of polycystic kidney disease. *Proc Natl Acad Sci U S A* 104(11):4389-4394.

6. Chen D*, et al.* (2014) Triptolide-containing formulation in patients with autosomal dominant polycystic kidney disease and proteinuria: an uncontrolled trial. *Am J Kidney Dis* 63(6):1070-1072.

7. Zhang J*, et al.* (2020) Triptolide attenuates renal damage by limiting inflammatory responses in DOCA-salt hypertension. *Int Immunopharmacol* 89(Pt A):107035.

8. Yuan XP, He XS, Wang CX, Liu LS, & Fu Q (2011) Triptolide attenuates renal interstitial fibrosis in rats with unilateral ureteral obstruction. *Nephrology (Carlton)* 16(2):200-210.

9. Zhou X*, et al.* (2016) Enhancer of Zeste Homolog 2 Inhibition Attenuates Renal Fibrosis by Maintaining Smad7 and Phosphatase and Tensin Homolog Expression. *J*

Am Soc Nephrol 27(7):2092-2108.

10. Zhang Y, Reif G, & Wallace DP (2020) Extracellular matrix, integrins, and focal adhesion signaling in polycystic kidney disease. *Cell Signal* 72:109646.

11. Bhunia AK, *et al.* (2002) PKD1 induces p21(waf1) and regulation of the cell cycle via direct activation of the JAK-STAT signaling pathway in a process requiring PKD2. *Cell* 109(2):157-168.

12. Takakura A, *et al.* (2009) Renal injury is a third hit promoting rapid development of adult polycystic kidney disease. *Hum Mol Genet* 18(14):2523-2531.

13. Weimbs T (2011) Third-hit signaling in renal cyst formation. *J Am Soc Nephrol* 22(5):793-795.

14. Prasad S, McDaid JP, Tam FW, Haylor JL, & Ong AC (2009) Pkd2 dosage influences cellular repair responses following ischemia-reperfusion injury. *Am J Pathol* 175(4):1493-1503.

15. Obermuller N, *et al.* (2002) Altered expression pattern of polycystin-2 in acute and chronic renal tubular diseases. *J Am Soc Nephrol* 13(7):1855-1864.

16. Harris PC (1999) Autosomal dominant polycystic kidney disease: clues to pathogenesis. *Hum Mol Genet* 8(10):1861-1866.

17. Dong K, *et al.* (2021) Renal plasticity revealed through reversal of polycystic kidney disease in mice. *Nat Genet* 53(12):1649-1663.

18. Li T, Yu C, & Zhuang S (2021) Histone Methyltransferase EZH2: A Potential Therapeutic Target for Kidney Diseases. *Front Physiol* 12:640700.

19. Su Z, *et al.* (2014) Excessive activation of the alternative complement pathway in

autosomal dominant polycystic kidney disease. *J Intern Med* 276(5):470-485.

20. Sun Y, *et al.* (2019) Activation of P-TEFb by cAMP-PKA signaling in autosomal dominant polycystic kidney disease. *Sci Adv* 5(6):eaaw3593.

21. Yin J, *et al.* (2015) Ezh2 regulates differentiation and function of natural killer cells through histone methyltransferase activity. *Proceedings of the National Academy of Sciences of the United States of America* 112(52):15988-15993.

22. Kim I, *et al.* (2009) Conditional mutation of Pkd2 causes cystogenesis and upregulates beta-catenin. *J Am Soc Nephrol* 20(12):2556-2569.

Figure legends

Fig. 1. Polycystin-2 is up-regulated in fibrotic kidneys.
(A) The time course of polycystin-2 expression in sham or unilateral ureteral obstruction (UUO) kidneys from wide type (WT) mice. The expression of collagen-I and polycystin-2 were analyzed by Western blotting and quantified. One representative of at least three independent experiments is shown. (B) The time course of polycystin-2 expression in unilateral ischemia-reperfusion injury (UIRI) kidneys from WT mice. The expression of collagen-I and polycystin-2 were analyzed by Western blotting and quantified. One representative of at least three independent experiments is shown. (C) The time course of polycystin-2 expression in aristolochic acid nephropathy (AAN) kidneys from WT mice. The expression of collagen-I and polycystin-2 in normal saline (NS) or AAN kidneys were analyzed by Western blotting and quantified. One representative of at least three independent experiments is shown.

Fig. 2. Triptolide inhibits the expression of polycystin-2 and attenuates renal fibrosis in mouse fibrotic kidneys.
WT mice received sham or UUO operation, which were followed by treatment with vehicle or triptolide for 10 days and were sacrificed at day 10. (A) Renal fibrosis was assessed by Masson's trichrome staining. Scale bar represents 100 μm. (B and C) The expression of collagen-I, phosphorylated Smad3 (pSmad3), a-SMA and polycystin-2 were analyzed by Western blotting. One representative of at least three independent experiments is shown. Wide type c57 mice underwent sham or UIRI operation, which were followed by treatment with vehicle or triptolide for 10 days starting from day 1. Mice were sacrificed at day 11. (D) Renal fibrosis was assessed by Masson's trichrome staining. (E and F) The expression of collagen-I, a-SMA and polycystin-2 were analyzed by Western blotting. One representative of at least three independent experiments is shown.

Fig. 3. Triptolide inhibit the expression of pro-fibrotic markers through polycystin-2 in fibrotic kidney cells.
(A) HK2 human renal epithelial cells were stimulated with TGF-β and treated with different concentration of triptolide for 48 hours. Cell lysates were collected, and Western blot analysis was performed to measure the expression of polycystin-2, fibronectin, N-cadherin, vimentin, and pSmad3. (B) normal rat renal fibroblasts (NRF-49F) were treated with different concentration of triptolide for 24 hours. Cell lysates were collected, and Western blot analysis was performed to measure the expression of polycystin-2, fibronectin, N-cadherin, and vimentin. (C) HK2 human renal epithelial cells were transfected with nonsense control (NC) or PKD2 siRNA (siPKD2). After 24h, cell lysates were collected, and Western blot analysis was performed to measure the expression of polycystin-2, fibronectin, N-cadherin, vimentin, and pSmad3. (D) HK2 cells were transfected with NC or PKD2 siRNA. On the second day, HK2 cells were stimulated with TGF-β for 48 hours. Cell lysates were

collected, and Western blot analysis was performed to measure the expression of polycystin-2, fibronectin, N-cadherin, vimentin, and pSmad3. (E) HK2 cells were transfected with NC or PKD2 siRNA. On the second day, HK2 cells were stimulated with TGF-β and treated with triptolide for 48 hours. Cell lysates were collected, and Western blot analysis was performed to measure the expression of polycystin-2, fibronectin, N-cadherin, vimentin, and pSmad3.

Fig. 4. Genetic deletion of *Pkd2* attenuates renal fibrosis in UUO kidneys.
Control (*Pkd2*$^{fl/+}$*;Cre/Esr1*$^{-}$), heterozygous (*Pkd2*$^{fl/+}$*;Cre/Esr1*$^{+}$) or homozygous (*Pkd2*$^{fl/fl}$*;Cre/Esr1*$^{+}$) *Pkd2* conditional knockout mice received sham or UUO operation and were sacrificed at day 14. (A) Renal fibrosis was assessed by Masson's trichrome staining. Scale bar represents 100 μm. (B) The expression of collagen-I, pSmad3, a-SMA and polycystin-2 were analyzed by Western blotting. One representative of at least three independent experiments is shown.

Fig. 5. Genetic deletion of *Pkd1* attenuates renal fibrosis in injured kidneys induced by UUO operation or folic acid injection.
(A) The time course of polycystin-1 expression in sham or UUO kidneys from WT mice. The expression of polycystin-1 was analyzed by Western blotting and quantified. One representative of at least three independent experiments is shown. Control (*Pkd1*$^{fl/+}$*;Cre/Esr1*$^{-}$), heterozygous (*Pkd1*$^{fl/+}$*;Cre/Esr1*$^{+}$) or homozygous (*Pkd1*$^{fl/fl}$*;Cre/Esr1*$^{+}$) *Pkd1* knockout mice received sham or UUO operation and were sacrificed at day 14. (A) Renal fibrosis was assessed by Masson's trichrome staining. Scale bar represents 100 μm. (B) The expression of collagen-I, pSmad3, a-SMA and polycystin-1 were analyzed by Western blotting. One representative of at least three independent experiments is shown. Control (*Pkd1*$^{fl/+}$*;Cre/Esr1*$^{-}$) or heterozygous (*Pkd1*$^{fl/+}$*;Cre/Esr1*$^{+}$) *Pkd1* knockout mice were injected with vehicle or folic acid (FA) intraperitoneally and were sacrificed at 48h. (C) Renal fibrosis was assessed by Masson's trichrome staining. Scale bar represents 100 μm. (D) The expression of collagen-I, pSmad3 and a-SMA were analyzed by Western blotting. One representative of at least three independent experiments is shown.

Fig. 6. Knockout of *Ezh2* abolished anti-fibrotic effect of *Pkd1* deletion in UUO kidneys.
(A) The expression of EZH2 were analyzed by Western blotting in *Pkd2* or *Pkd1* knockout mice after UUO operation or FA injection. One representative of at least three independent experiments is shown. Control (*Ezh2*$^{+/+}$*;Pkd1* $^{fl/fl}$*;Cre/Esr1*$^{-}$), *Ezh2* (*Ezh2*$^{fl/fl}$*;Pkd1*$^{+/+}$*;Cre/Esr1*$^{+}$), *Pkd1* (*Ezh2*$^{+/+}$*; Pkd1*$^{fl/fl}$*;Cre/Esr1*$^{+}$) or *Pkd1/EZH2* (*Ezh2*$^{fl/fl}$*;Pkd1*$^{fl/fl}$*;Cre/Esr1*$^{+}$) knockout mice received UUO operation and were sacrificed at day 14. (B) Renal fibrosis was assessed by Masson's trichrome staining. Scale bar represents 100 μm. (C) The expression of collagen-I, pSmad3, a-SMA, EZH2 and polycystin-1 were analyzed by Western blotting. One representative of at least three independent experiments is shown.

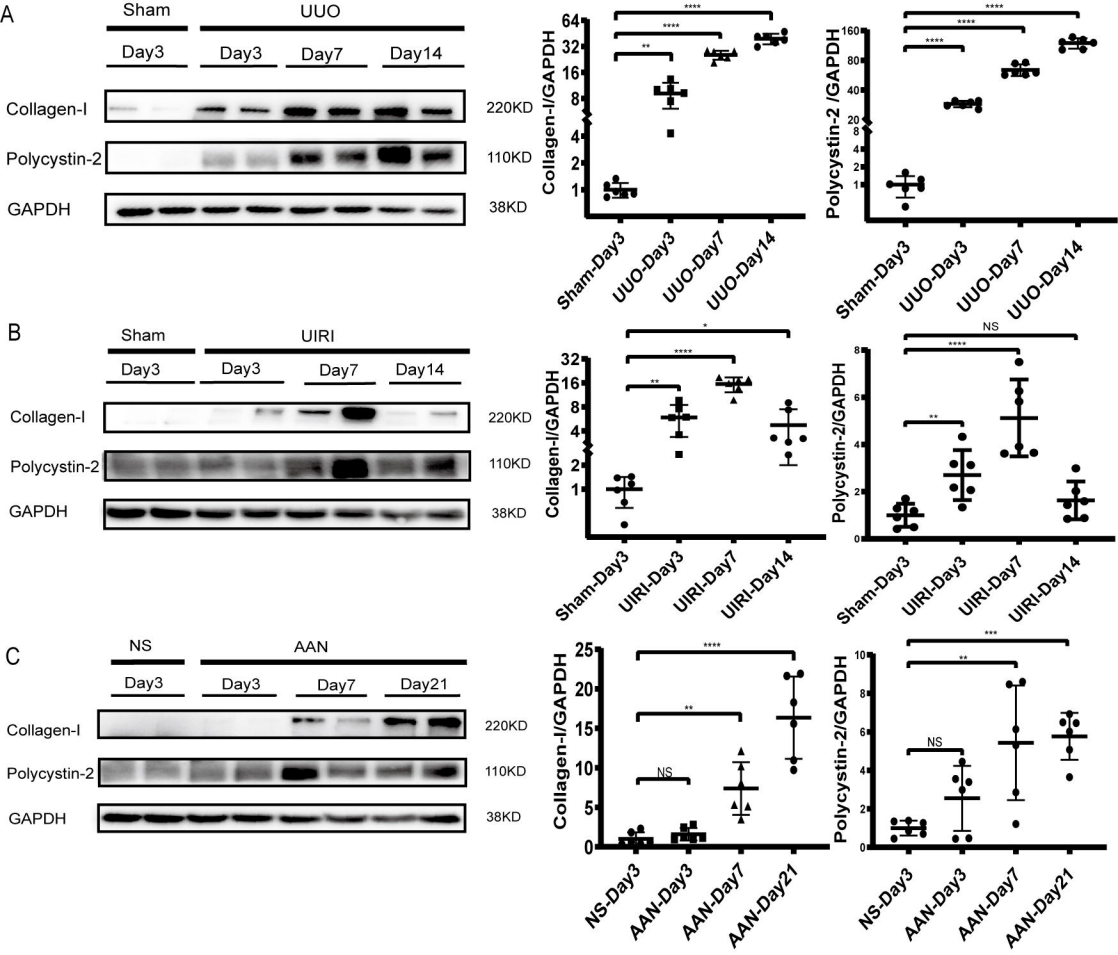
A
Sham
UUO
Day3
Day3
Day7
Day14
Collagen-I
Polycystin-2
GAPDH
220KD
110KD
38KD
Collagen-I/GAPDH
Polycystin-2 /GAPDH
Sham-Day3
UUO-Day3
UUO-Day7
UUO-Day14
B
Sham
UIRI
Day3
Day3
Day7
Day14
Collagen-I
Polycystin-2
GAPDH
220KD
110KD
38KD
Collagen-I/GAPDH
Polycystin-2/GAPDH
NS
Sham-Day3
UIRI-Day3
UIRI-Day7
UIRI-Day14
C
NS
AAN
Day3
Day3
Day7
Day21
Collagen-I
Polycystin-2
GAPDH
220KD
110KD
38KD
Collagen-I/GAPDH
Polycystin-2/GAPDH
NS
NS-Day3
AAN-Day3
AAN-Day7
AAN-Day21

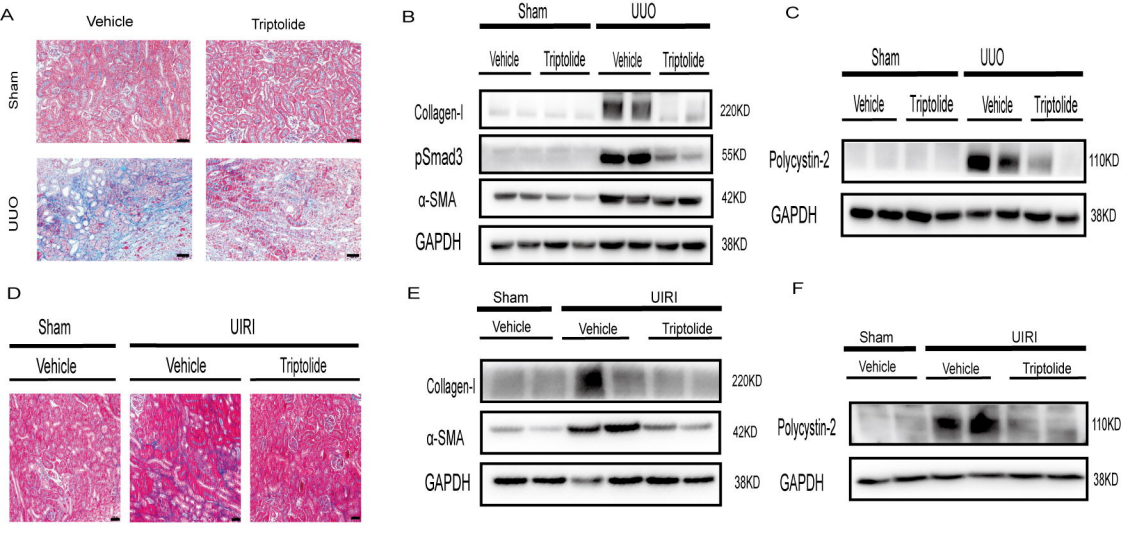
A
Vehicle
Triptolide
Sham
UUO
B
Sham
UUO
Vehicle
Triptolide
Vehicle
Triptolide
Collagen-I
220KD
pSmad3
55KD
α-SMA
42KD
GAPDH
38KD
C
Sham
UUO
Vehicle
Triptolide
Vehicle
Triptolide
Polycystin-2
110KD
GAPDH
38KD
D
Sham
UIRI
Vehicle
Vehicle
Triptolide
E
Sham
UIRI
Vehicle
Vehicle
Triptolide
Collagen-I
220KD
α-SMA
42KD
GAPDH
38KD
F
Sham
UIRI
Vehicle
Vehicle
Triptolide
Polycystin-2
110KD
GAPDH
38KD

A

HK2 Cells

Ctr | TGF-β

DMSO | DMSO | Triptolide 10nM | Triptolide 100nM | Triptolide 1000nM

Fibronectin 275KD

N-cadherin 135KD

pSmad3 55KD

Vimetin 53KD

GAPDH 38KD

HK2 Cells

Ctr | TGF-β

DMSO | DMSO | Triptolide 10nM | Triptolide 100nM | Triptolide 1000nM

Polycystin-2 110KD

GAPDH 38KD

B

NRK-49F Cells

DMSO | Triptolide 10nM | Triptolide 100nM | Triptolide 1000nM

Fibronectin 275KD

N-cadherin 135KD

Vimetin 53KD

GAPDH 38KD

NRK-49F Cells

DMSO | Triptolide 10nM | Triptolide 100nM | Triptolide 1000nM

Polycystin-2 110KD

GAPDH 38KD

C

HK2 Cells

NC | siPKD2

Fibronectin 275KD

N-cadherin 135KD

pSmad3 55KD

Vimetin 53KD

GAPDH 38KD

HK2 Cells

NC | siPKD2

Polycystin-2 110KD

GAPDH 38KD

D

HK2 Cells

Ctr | TGF-β

NC | NC | siPKD2

Fibronectin 275KD

N-cadherin 135KD

pSmad3 55KD

Vimetin 53KD

GAPDH 38KD

HK2 Cells

Ctr | TGF-β

NC | NC | siPKD2

Polycystin-2 110KD

GAPDH 38KD

E

HK2 Cells

NC | siPKD2

DMSO | Triptolide | DMSO | Triptolide

Fibronectin 275KD

N-cadherin 135KD

pSmad3 55KD

Vimetin 53KD

GAPDH 38KD

HK2 Cells

NC | siPKD2

DMSO | Triptolide | DMSO | Triptolide

Polycystin-2 110KD

GAPDH 38KD

A

	Sham	UUO		
	Pkd2$^{fl/+}$	Pkd2$^{fl/+}$	Pkd2$^{fl/+}$	Pkd2$^{fl/fl}$
Cre	—	—	+	+

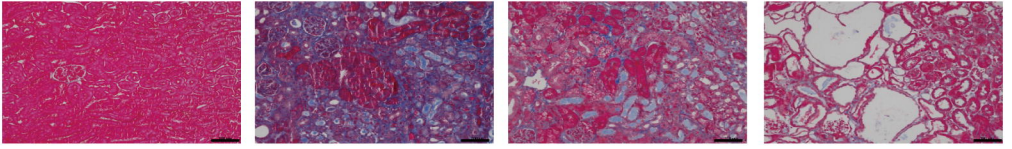

B

	Sham	UUO		
	Pkd2$^{fl/+}$	Pkd2$^{fl/+}$	Pkd2$^{fl/+}$	Pkd2$^{fl/fl}$
Cre	—	—	+	+

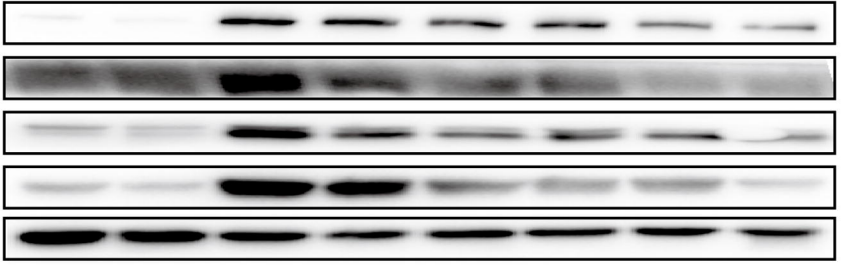

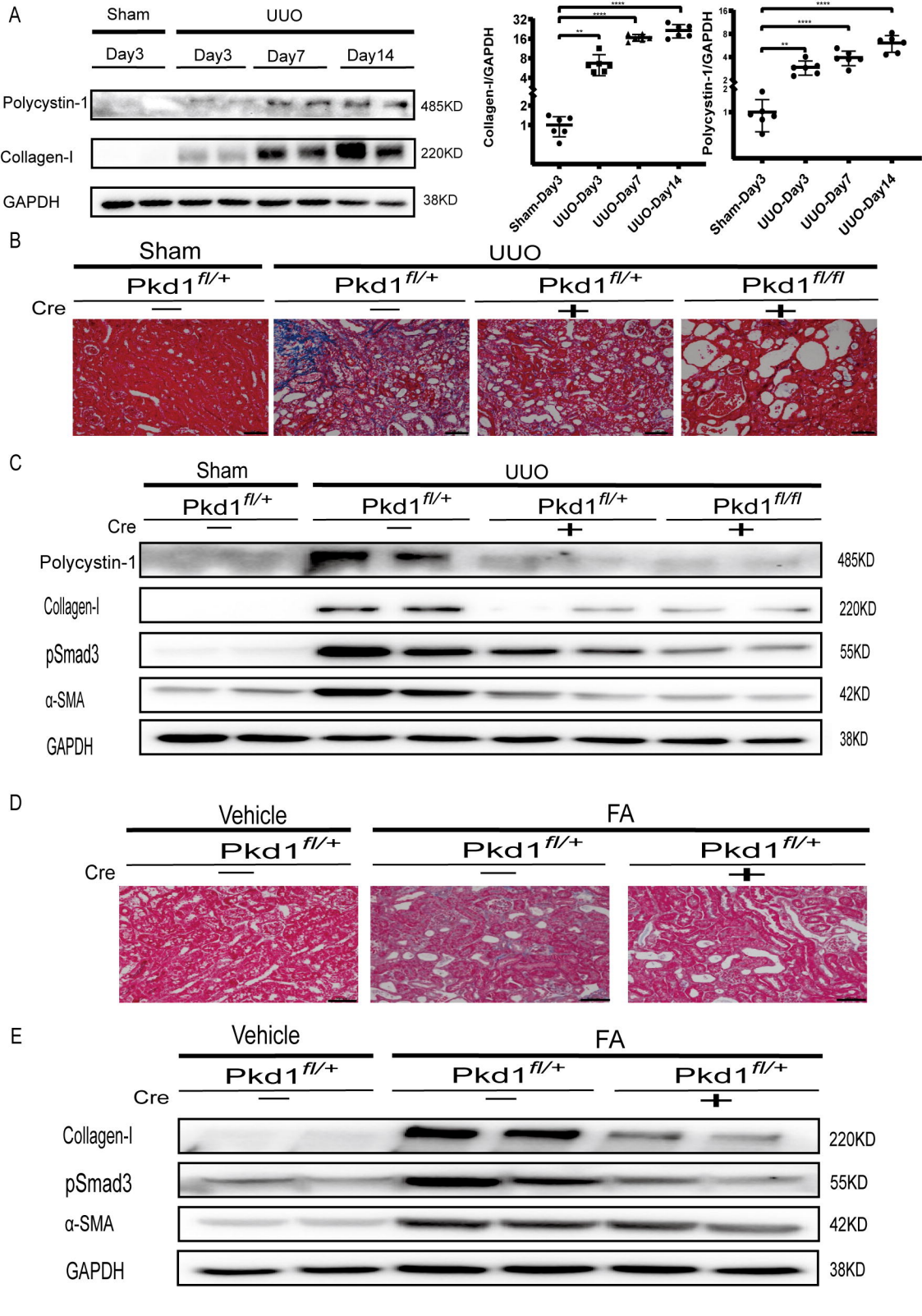
A
Sham
UUO
Day3
Day3
Day7
Day14
Polycystin-1
Collagen-I
GAPDH
485KD
220KD
38KD
Collagen-I/GAPDH
Polycystin-1/GAPDH
Sham-Day3
UUO-Day3
UUO-Day7
UUO-Day14
B
Sham
UUO
Pkd1fl/+
Pkd1fl/+
Pkd1fl/+
Pkd1fl/fl
Cre
C
Sham
UUO
Pkd1fl/+
Pkd1fl/+
Pkd1fl/+
Pkd1fl/fl
Cre
Polycystin-1
Collagen-I
pSmad3
α-SMA
GAPDH
485KD
220KD
55KD
42KD
38KD
D
Vehicle
FA
Pkd1fl/+
Pkd1fl/+
Pkd1fl/+
Cre
E
Vehicle
FA
Pkd1fl/+
Pkd1fl/+
Pkd1fl/+
Cre
Collagen-I
pSmad3
α-SMA
GAPDH
220KD
55KD
42KD
38KD

A

Sham | UUO

Pkd2$^{fl/+}$ | Pkd2$^{fl/+}$ | Pkd2$^{fl/+}$ | Pkd2$^{fl/fl}$

Cre — — + +

EZH2 98KD

GAPDH 38KD

B

Sham | UUO

Pkd1$^{fl/+}$ | Pkd1$^{fl/+}$ | Pkd1$^{fl/+}$ | Pkd1$^{fl/fl}$

Cre — — + +

EZH2 98KD

GAPDH 38KD

C

Vehicle | FA

Pkd1$^{fl/+}$ | Pkd1$^{fl/+}$ | Pkd1$^{fl/+}$

Cre — — +

EZH2 98KD

GAPDH 38KD

D

UUO

Pkd1$^{fl/fl}$ EZH2$^{+/+}$ | Pkd1$^{fl/fl}$ EZH2$^{+/+}$ | Pkd1$^{+/+}$ EZH2$^{fl/fl}$ | Pkd1$^{fl/fl}$ EZH2$^{fl/fl}$

Cre — + + +

E

UUO

Pkd1$^{fl/fl}$ EZH2$^{+/+}$ | Pkd1$^{fl/fl}$ EZH2$^{+/+}$ | Pkd1$^{+/+}$ EZH2$^{fl/fl}$ | Pkd1$^{fl/fl}$ EZH2$^{fl/fl}$

Cre — + + +

Polycystin-1 485KD

Collagen-I 220KD

EZH2 98KD

pSmad3 55KD

α-SMA 42KD

GAPDH 38KD